Spin-polarized electron liquid at arbitrary temperatures: Exchange-correlation energies, electron-distribution functions, and the static response functions

François Perrot
Centre d'Etudes de Bruyères le Châtel, P.O. Box 12, 91689 Bruyères le Châtel, France

M. W. C. Dharma-wardana*
National Research Council, Ottawa, Canada K1A 0R6
(Received 31 March 2000)

We use a recently introduced classical mapping of the Coulomb interactions in a quantum electron liquid [Phys. Rev. Lett. **84**, 959 (2000)] to present a unified treatment of the thermodynamic properties and the static response of the *finite-temperature* electron liquid, valid for arbitrary coupling and spin-polarization. The method is based on using a ''quantum temperature'' T_q such that the distribution functions of the *classical* electron liquid at T_q leads to the same correlation energy as the quantum electron liquid at $T=0$. The functional form of $T_q(r_s)$ is presented. The electron-electron pair-distribution functions (PDF's) calculated using T_q are in good quantitative agreement with available $(T=0)$ quantum Monte Carlo results. The method provides a means of treating strong-coupling regimes of n,T, and ζ currently unexplored by quantum Monte Carlo or Feenberg-functional methods. The exchange-correlation free energies, distribution functions $g_{11}(r)$, $g_{12}(r)$, $g_{22}(r)$ and the local-field corrections to the static response functions as a function of density n, temperature T, and spin polarization ζ are presented and compared with any available finite-T results. The exchange-correlation free energy $f_{xc}(n,T,\zeta)$, is given in a parametrized form. It satisfies the expected analytic behavior in various limits of temperature, density, and spin polarization, and can be used for calculating other properties like the equation of state, the exchange-correlation potentials, compressibility, etc. The static local-field correction provides a static response function which is consistent with the PDF's and the relevant sum rules. Finally, we use the finite-T xc-potentials to examine the Kohn-Sham bound- and continuum states at an Al^{13+} nucleus immersed in a hot electron gas to show the significance of the xc-potentials.

I. INTRODUCTION

Recent advances in materials science, experiments using intense lasers, etc., have created a need for improved theoretical tools for treating electronic systems at arbitrary (strong) coupling and for a wide range of densities and temperatures. Similarly, electrons and other fermions in astrophysical plasmas, white dwarfs, etc.,[1] are at densities and temperatures such that they range from full degeneracy to high-temperature Maxwellian distributions. The Maxwellian limit of the uniform electron gas (UEG) is usually studied under the name ''one-component plasma'' (OCP). Since it is a classical system, its properties have been studied extensively using integral-equations methods as well as classical simulations.[2,3] The zero-temperature UEG is generally sufficient for metal physics, and has been the object of an enormous effort. The UEG at finite T is important not only for the reasons already mentioned, but also because it provides a model exchange-correlation potential for the density-functional theory (DFT) of finite-T inhomogeneous electronic systems.[4,5] Many other applications of the finite-T UEG arise in understanding new materials,[6] doped semiconductors and nanostructures, as well as with respect to the older topics like liquid metals, etc., discussed some time ago in Ref. 8. Recent studies on compressed hydrogen,[7] both in the solid and liquid phase, have demonstrated the need to treat the protons on an equal footing with the electrons and the methods discussed here should be of interest.

The Hartree-Fock approximation,[9] and the random-phase approximation (RPA) provide useful ''benchmarks'' for calculations of the properties of the interacting UEG at finite T.[10–13] RPA is a reasonable approximation when the ''coupling parameter'' Γ, the ratio of the potential energy to the kinetic energy of the Coulomb fluid, is smaller than unity. The Γ for the UEG at $T=0$ reduces to the mean-sphere radius r_s per electron, i.e., for the three-dimensional (3D) case, $\Gamma=r_s=(3/4\pi n)^{1/3}$, with n the number density per a.u. Since electronic interactions involve exchange effects, the spin-polarization $\zeta=(n_1-n_2)/n$, where n_i is the number density of spin species i of the system, brings in a multicomponent aspect to the theory. The RPA holds in the high-temperature low-density limit where it reduces to Debye-Hükel theory, and in the $T=0$ high-density limit, since these are both weak-coupling regimes. However, for typical regimes of physical interest, the electron-electron pair-distribution functions (PDF's), $g(r_s,r)$, calculated in the RPA are not found to be positive definite. Improving the RPA is nontrivial if the theory is expected to satisfy sum rules and provide physically realistic $g(r)$. Diagrammatic methods look for resummations that conserve the sum rules, Ward identities, etc.[14–17] These methods become quite unwieldy for finite-T strong coupling. Hence most attempts to go beyond the weak-coupling regime are based on the construction of local-field corrections (LFC's) to the RPA response functions.[8,18–22] The equations of motion (EQM) of the density operator beyond the RPA require an ''ansatz'' to ''close'' the equations. Singwi *et al.* (STLS), used a physically-motivated closure by introducing the electron

PDF determined self-consistently.[18] A finite-T application of STLS was given by Tanaka *et al.*[21] The STLS-type method was also used by the Cornell group (Ref. 8), in the form of a finite-T extension of the Vashista and Singwi (VS) approach at $T=0$.[19] They provided parametrized forms for the exchange-correlation free energy f_{xc} and various thermodynamic properties of the UEG without spin polarization. Comprehensive studies of the finite-T electron fluid were presented by Ichimaru and collaborators. They used extensions of the STLS method as well as methods based on a modified-convolution approximation and provide parametrized forms for the spin-polarized UEG.[21–23] All these treatments do not overcome the underlying difficulty that the $g(r)$ becomes negative for some values of r, for sufficiently large r_s (e.g., $r_s \sim 5$, or even 2 in some cases) in the metallic range, although the situation is much improved compared to RPA. Further, very often the small-k and large-k limits of the model LFC's used in these theories are fitted to *ad hoc* values or values obtained from theoretical results *outside* the method used. Nevertheless, these methods have been more successful than straight diagrammatic methods in obtaining practical results for the regime beyond weak coupling, especially because the energy could be calculated with good accuracy even if the PDF's were unsatisfactory.

Another approach, well known in $T=0$ applications, assumes a trial wave function of the form $\psi=FD$, where F is a correlation factor and D is a Slater determinant. This typically leads to the Feenberg energy functionals which are handled in several ways.[24–26] Quantum Monte Carlo (QMC) techniques also use such a ψ and lead, e.g., to the variational Monte Carlo (VMC) method.[27–30] The QMC estimate of the exchange-correlation energy, $E_{xc}(r_s)$, at $T=0$ is now available in several parametrized forms.[28,32,33] While it is easy to get good $E_{xc}(r_s)$, the opposite is true for other properties like the PDF's and LFC's. There is at present a very considerable interest in extending these methods for the UEG at finite T and ζ, as well as for dense hydrogen.[34]

In a recent letter we showed that the many-body interactions in the $T=0$ UEG are such that its static properties, e.g., $g(r)$, $E_{xc}(r_s,\zeta)$, static LFC's, may be extracted from a study of the *classical* Coulomb fluid at a ''quantum'' temperature T_q, and presented a parametrization of T_q as a function of r_s.[35] In parallel with the Fermi-hypernetted-chain and Bose-hypernetted-chain methods, we will call this a classical-map hypernetted-chain method, (CHNC), although of course, the HNC is *ipso facto* a classical method. Other classical integral equations or molecular dynamics may of course be used instead of the HNC, within the classical map presented here, and in Ref. 35. In this study we extend the CHNC calculations to the finite-temperature electron liquid, assuming that the same conceptual basis holds here. At $T=0$, the method could be checked against results from QMC and other studies. At finite T we do not have QMC results, but a variety of previous studies as well as the behavior at various limiting situations of r_s, T, and ζ are available to provide a check on the methods used. In Sec. II we review the classical map for quantum electrons for the convenience of the reader and provide additional results for the $T=0$ case not reported in our previous publication, viz., Ref. 35. In Sec. III we present results for the pair-distribution functions of the finite-T electron gas. The parametrized form of the exchange-correlation free energy and several derived properties are presented in Sec. IV. The local-field corrections to the static response at finite-T are discussed in Sec. V. In Sec. VI we use the new xc-potentials to study the Kohn-Sham electronic structure of an Al-ion immersed in a hot electron gas and show that there are significant differences from the results obtained from the Iyetomi-Ichimaru xc-potential.

II. THE CLASSICAL MAP FOR QUANTUM ELECTRONS

The thermodynamics and static-response functions of a system of interacting particles can be calculated if the pair-distribution functions and the interaction potentials are known. The PDF's of classical fluids are easily obtainable from classical Monte Carlo simulations or using the hypernetted-chain (HNC) equation and its extensions.[36] We use the HNC method in our work as it is not computer intensive and also provides a formal language suitable for conceptual analysis. In Ref. 35 we showed that there exists a temperature T_q such that, at that temperature, the PDF's of a *classical* Coulomb fluid are in very close agreement with the PDF's of the *quantum* electron gas and yield the same correlation energy. In effect, we asked for the temperature T_q at which the PDF's of a Coulomb fluid, obeying the *classical* HNC-integral equation, yielded the E_c of the UEG at the same density and at $T=0$. The suffix q in T_q signifies that this temperature reflects the quantum many-body interactions in the UEG. Using the temperature T_q at each r_s we obtained $g_{ij}(r)$, spin-polarized correlation energies $E_c(r_s,\zeta)$, LCF's etc., for the $T=0$ case.

The physical motivation for our method comes from DFT where interacting electrons are replaced by noninteracting Kohn-Sham (KS) particles whose wave function is a simple determinant. This is conceptually very different to the Feenberg approach which uses a correlated wave function of the form $\psi=FD$.[25,26] In DFT, the many-body potential is replaced by a one-body KS potential, V_{KS}, obtained from the exchange-correlation energy E_{xc}. Since the natural energy parameter of the classical ensemble is the temperature, we look for a temperature mapping of the E_{xc}.

Our objective is to construct a classical Coulomb fluid at some temperature T_{cf} such that its correlation energy and spin-dependent distribution functions are those of a quantum electron gas at some given temperature T. Consider a fluid of mean density n containing two spin species with concentrations $x_i=n_i/n$. We deal with the physical temperature T of the UEG, while the temperature of the classical fluid T_{cf} is $1/\beta_{cf}$. Since the leading dependence of the energy on temperature is quadratic, we assume that a suitable formula interpolating between the low-T and high-T regimes is given by $T_{cf}=\sqrt{(T^2+T_q^2)}$. This is clearly valid for $T=0$ and for high T. The case $T=0$ was examined in Ref. 35 where T_q was determined as a function of r_s, and the agreement between the quantum pair distributions with those calculated from the classical model was established in detail. In this study we present detailed calculations at finite-T using our quadratic interpolation. A physical interpretation of T_{cf} is given in Appendix A, where it is shown to agree with the classical temperature which gives the correct quantum kinetic energy per electron. Comparison with results from other available methods suggests that it provides a suitable

interpolation for all T, while being valid for low-T and high-T regimes by construction. At this point we may note that *every single* theory of the finite-T electron liquid that attempts to provide numerical results that go beyond RPA are essentially based on some *assumed* interpolation between the $T=0$ and high-T regimes. Thus Tanaka *et al.*,[22] interpolate between two types of modified-convolution approximations, while ours is between two regimes of the HNC equation. The method of Dandrea *et al.*,[8] uses the STLS ''ansatz,'' assumes that the Vashista-Singwi static LFC can be used with interpolations (unspecified in the paper) of the compressibility between the $T=0$ and high-T limits, and carry out frequency integrations over the static LFC's. Since the compressibility is related to the density gradient of the xc-potentials, using the compressibility as an input clearly poses some questions. The results are justified by DAC by noting that their ''calculations of the excess free energy of the intermediate degeneracy regime find good agreement with the more exact results of Tanaka *et al.*'' In a similar sense, the validation of our interpolation procedure is based on the general consistency of our results with previous methods, as well as the positivity and other favorable aspects of our pair-distributions functions, other properties etc., that we present in this work, but not found in other methods. A more complete validation of the results from existing theories of the finite-T UEG, including ours, has to await results from complementary methods which use different assumptions (e.g., stochastic simulations).

The pair-distribution functions for a classical fluid at an inverse temperature β_{cf} can be written as

$$g_{ij}(r)=e^{[-\beta_{cf}\phi_{ij}(r)+h_{ij}(r)-c_{ij}(r)+B_{ij}(r)]}. \tag{1}$$

Here $\phi_{ij}(r)$ is the pair potential between the species i,j. For two electrons this is just the Coulomb potential $V_{cou}(r)$. If the spins are parallel, the Pauli principle prevents them from occupying the same spatial orbital. Following earlier work, notably by Lado,[37] we also introduce a ''Pauli potential,'' $\mathcal{P}(r)$. Thus $\phi_{ij}(r)$ becomes $\mathcal{P}(r)\delta_{ij}+V_{cou}(r)$.

$$\phi_{ij}(r)=\mathcal{P}(r)\delta_{ij}+V_{cou}(r). \tag{2}$$

The Pauli potential $\mathcal{P}(r)$ will be discussed with the PDF's of the noninteracting UEG, i.e., $g^0_{ij}(r)$. The function $h(r)$ is $g(r)-1$; it is related to the structure factor $S(k)$ by a Fourier transform. The $c(r)$ is the ''direct correlation function (DCF)'' of the Ornstein-Zernike (OZ) equations:

$$h_{ij}(r)=c_{ij}(r)+\Sigma_s n_s\int d\mathbf{r}'\,h_{i,s}(|\mathbf{r}-\mathbf{r}'|)c_{s,j}(\mathbf{r}'). \tag{3}$$

The $B_{ij}(r)$ term in Eq. (1) is the ''bridge'' term arising from certain cluster interactions. If this is neglected Eqs. (1)–(3) form a closed set providing the HNC approximation to the PDF of a classical fluid. Various studies have clarified the role of $B(r)$ and its treatment via ''reference'' HNC equations.[38] $B(r)$ is important when the coupling constant Γ exceeds, say, 20. The range of Γ relevant to this work can be estimated once T_q is known. Thus, using the results from Ref. 35, $\Gamma\sim 4.5$, ~ 7.2 and ~ 15.2 for $r_s=10$, 20, and 50, respectively. Hence the HNC approximation holds in most cases of interest. In fact, in this study we consider the range $r_s\leqslant 10$ to construct the parametrized energy expressions. However, the robustness of the method is such that the correlation-energy estimates are found to be accurate even at $r_s=20$, i.e., well outside the fitted regime. The HNC approximation suffers from a compressibility inconsistency (CI), i.e., the excess compressibility calculated from the small-k limit of the short-ranged part of $c(k)$ does not agree with that obtained from the excess free energy. The RPA, Hubbard,[14] and also STLS methods suffer from such a CI even for coupling regimes much smaller than those where the HNC holds good. In fact, the Vashista-Singwi model was an attempt to correct the CI in the original STLS method and extend it to the metallic regime of r_s. The CI in the HNC scheme can be corrected by including a suitable bridge term. In this study we retain the simple-HNC scheme since the range of Γ involved is such that the CI is not at all serious.

Consider the noninteracting system at temperature T, with $x_i=0.5$ for the paramagnetic case. The parallel-spin PDF, i.e., $g^0_{ii}(r,T)$, will be denoted by $g^0_T(r)$ for simplicity, since $g^0_{ij}(r,T)$, $i\neq j$ is unity. Denoting $(\mathbf{r}_1-\mathbf{r}_2)$ by $\mathbf{r}$, it is easy to show that

$$g^0_T(\mathbf{r})=\frac{2}{N^2}\Sigma_{\mathbf{k}_1,\mathbf{k}_2}n(k_1)n(k_2)[1-e^{i(\mathbf{k}_1-\mathbf{k}_2)\cdot\mathbf{r}}]. \tag{4}$$

Here $n(k)$ is the Fermi occupation number at the temperature T. Equation (4) reduces to

$$g^0_T(r)=1-F^2_T(r) \tag{5}$$

$$F_T(r)=(6\pi^2/k_F^3)\int n(k)\frac{\sin(kr)}{r}\frac{kdk}{2\pi^2}. \tag{6}$$

Here k_F is the Fermi momentum. Thus $g^0_T(r)$ is obtained from the Fourier transform of the Fermi function. Then $c^0(r)$ can be evaluated from $g^0_T(r)$ using the OZ relations. The $T=0$ case can be evaluated analytically.[37] Assuming that $g^0_{ii}(r)$ can be modeled by an HNC fluid with the pair interaction $\beta_{cf}\mathcal{P}(r)$ (and dropping the indices), we have

$$g^0(r)=exp[-\beta_{cf}\mathcal{P}(r)+h^0(r)-c^0(r)]. \tag{7}$$

The k-space DCF, i.e., $c^0(k)$, decays as $4k_F/3k$ for small k and for $T=0$, showing that the r-space form $c^0(r)$ is long ranged. The ''Pauli potential'' $\mathcal{P}(r)$ is given by

$$\beta\mathcal{P}(r)=-\log[g^0(r)]+h^0(r)-c^0(r). \tag{8}$$

We can determine only the product $\beta_{cf}\mathcal{P}(r)$. The ''classical-fluid temperature'' $1/\beta_{cf}$ is still undefined and is *not* the thermodynamic temperature T. The Pauli potential is a universal function of rk_F at $T=0$. It is long ranged and mimics the exclusion effects of Fermi statistics. At finite T its range is about a thermal wavelength and is increasingly hard-sphere-like. Plots of $\beta\mathcal{P}(r)$ and related functions are given in Fig. 1 of Ref. 35.

The next step is to use the full pair potential $\phi_{ij}(r)$, and solve the coupled HNC and OZ equations for the binary (up and down spins) *interacting* fluid. For the paramagnetic case, $n_i=n/2$, we have:

$$g_{ij}(r)=e^{-\beta_{cf}(\mathcal{P}(r)\delta_{ij}+V_{cou}(r))+h_{ij}(r)-c_{ij}(r)}, \tag{9}$$

$$h_{ij}(q) \overset{\text{FT}}{=\!\!=\!\!\rightarrow} h_{ij}(r), \tag{10}$$

$$h_{11}(q) = c_{11}(q) + (n/2)\Sigma_\gamma c_{1\gamma}(q) h_{\gamma 1}(q), \tag{11}$$

$$h_{12}(q) = c_{12}(q) + (n/2)\Sigma_\gamma c_{1\gamma}(q) h_{\gamma 2}(q). \tag{12}$$

The Coulomb potential $V_{cou}(r)$ needs some discussion. For two point-charge electrons this is $1/r$. However, depending on the temperature T, an electron is localized to within a thermal wavelength. Thus, following Minoo, Gombert, and Deutsch,[39] we use a ''diffraction corrected'' form:

$$V_{cou}(r) = (1/r)[1 - e^{-r/\lambda_{th}}]; \quad \lambda_{th} = (2\pi \bar{m} T_{cf})^{-1/2}. \tag{13}$$

Here $\bar{m}$ is the reduced mass of the electron pair, i.e., $m^*(r_s)/2$ a.u., where $m^*(r_s)$ is the electron effective mass. It is weakly r_s dependent, e.g., ~ 0.96 for $r_s = 1$. In fact, it is also dependent on the spin-polarization ζ, and could be self-consistently determined from the $T \rightarrow 0$ limit of the interacting specific heat of the electron gas at the given r_s and ζ, predicted by the present theory itself. However, the results are not strongly sensitive to m^* and in this work we adopt the simplest procedure and take $m^* = 1$. The ''diffraction correction'' ensures the correct behavior of $g_{12}(r \sim 0)$ at ''contact'' for any given r_s. We shall return to the question of the contact value of $g(r)$ since there is a lot of interest and a wide literature on just the evaluation of $g_{12}(r = 0)$, because of its importance in LFC's, in DFT-gradient corrections and other applications.[40–42,44–46]

In solving the above equations for a given r_s and at $T = 0$, we have $T_{cf} = T_q$. A trial T_q is adjusted to obtain an $E_c(T_q)$ equal to the known *paramagnetic* $E_c(r_s)$ at each r_s, via a coupling constant integration. In effect, we determine T_q by requiring that the classical Coulomb fluid at T_q has the same correlation energy as the quantum UEG at $T = 0$. The resulting ''quantum'' temperatures $T_q(r_s)$ could be fitted to the form:

$$T_q/E_F = 1/(a + b\sqrt{r_s} + c r_s). \tag{14}$$

Note that $T_q(r_s)$ is equally well a parametrization of the correlation energy, viz., $T_q(E_c(r_s))$, or $E_c(T_q)$. The results for E_c from different QMC methods differ, e.g., by $\sim 6\%$ at $r_s = 1$. We used the recent Ortiz-Ballone E_c data for the paramagnetic UEG from VMC and DMC.[28] The difference in E_c in VMC and DMC leads to slightly different fits. The fit coefficients are, for DMC, $a = 1.594$, $b = -0.3160$, and $c = 0.0240$, while for VMC $a = 1.3251$, $b = -0.1779$, and $c = 0.0$. Eight values of r_s, viz., $r_s = 1 - 6$, 8, and 10 were used in the fit to T_q. At $r_s = 1$ and 10, T_q/E_F goes from 0.768 to 1.198. Although based on fits not exceeding $r_s = 10$, Eq. (14) turns out to be very robust in that it gives very good results at, e.g., $r_s = 20$. That is, we use Eq. (14) to predict T_q at $r_s = 20$ and use that T_q to predict an $e_c = E_c/n$ of -0.01144 a.u. per electron for the paramagnetic UEG, in comparison with the value of -0.0115 a.u. reported by Ortiz, Harris, and Ballone using DMC-QMC.[29] As $r_s \rightarrow 0$, $g(r)$ tends to $g^0(r)$. The UEG as $r_s \rightarrow 0$ goes to a high-density fluid interacting via the Pauli potential. For small r_s, standard perturbation methods are adequate and the techniques presented here are really not necessary.

The $T_q(r_s)$ function given by Eq. (14), suitably scaled, is of general applicability for all spin-half fermions interacting via a Coulomb potential. Thus it may be applied to a spin-1/2 gas of protons for which the a.u. length scale $\rightarrow$ a.u./M_H and the au.. energy scale $\rightarrow$ Hartree (M_H), where M_H is the mass of the proton. In contrast, it is not applicable to liquid He^3 since the rare-gas interaction is not Coulombic. The form of T_q applicable to liquid He^3 can be derived easily using the methods of Ref. 35 and the He-He pair potential.

The only quantum many-body input to this analysis is the *paramagnetic* $E_c(r_s)$ at $T = 0$. Since even theories which give PDF's which are not positive definite provide acceptable estimates of $E_c(r_s)$, our CHNC can be incorporated to any such method for obtaining a first prediction of a positive definite $g(r)$ within any such theory. It is found that the T_q, determined from the paramagnetic case (i.e, $\zeta = 0$), reproduces the QMC-correlation energies for other values of ζ at a given r_s. Thus T_q is essentially independent of ζ.

In applying this information to the finite-T electron liquid at a given density parameter r_s, we set the classical-fluid temperature T_{cf} to be equal to $(T_q^2 + T^2)^{1/2}$, with T_q given by Eq. (14). The xc-free energy per electron, $f_{xc}(r_s, T) = F_{xc}/n$, is equivalently $f_{xc}(T_q, T)$. It is evaluated from the distribution functions via the usual coupling-constant integration:

$$f_{xc} = \int_0^1 d\lambda \frac{n}{2} \int \frac{4\pi r^2 dr}{r} \sum_{ij} x_i x_j h_{ij}(r, \lambda). \tag{15}$$

In the paramagnetic case $x_i = x_j = 1/2$ and we have

$$f_{xc} = \int_0^1 \frac{d\lambda}{4} n \int \frac{4\pi r^2 dr}{r} [h_{11}(r, \lambda) + h_{12}(r, \lambda)]. \tag{16}$$

(f_x is obtained from the noninteracting system, $\lambda = 0$, where h_{11} and h_{12} become h_{11}^0 and h_{12}^0, respectively. Also, $h_{12}^0 = 0$ and there is no coupling-constant integration since λ is fixed at zero.)

Once $f_{xc}(r_s, T, \zeta)$ is determined, the thermodynamics of the electron liquid at any degeneracy and spin-polarization is known. The SPDF's $g_{ij}(r_s, T, \zeta)$ and the corresponding structure factors $S_{ij}(k)$ are also known. Since these are those of a classical fluid at a temperature T_{cf}, we can relate the $S_{ij}(k)$ to the interacting and noninteracting response functions as in Ref. 35. Thus the interacting response function as well as the LFC's are known as a function of r_s, T, and ζ. Hence the method provides a unified scheme for the thermodynamics and static response of the electron liquid for r_s, T, and ζ, without strong limitations on the coupling strength. Since we have used the HNC model which is essentially a fluid model, this approach will most probably not apply to regimes of r_s and T where Wigner crystallization begins to occur. In such regimes the HNC scheme would describe the metastable liquid phase. However, the methods presented here can be applied to a solid phase as well if the HNC approach is suitably modified or if classical simulations are used with the potentials of the classical map given here. Existing QMC studies have included spin-density wave and Wigner-crystallization regimes,[29] but essentially using the

correlated-determinantal form containing only a *single term* in the configuration-interaction expansion. Our study is restricted to the fluid regime only. The current $T_q(r_s)$ parametrization, Eq. (14) has been fitted for a maximum $r_s=10$, but as already noted, we get very good prediction of the correlation energy at $r_s=20$, which is within the spin-density wave regime. A study of the phase diagram will not be undertaken in this study, although it is of topical interest.[6]

III. PAIR-DISTRIBUTION FUNCTIONS AT FINITE *T*

Compared to previous methods of dealing with interacting electrons at zero and finite T, the classical mapping to the HNC equation presented in this study provides reliable calculations of the pair-distribution functions which are guaranteed to be positive definite at any r_s, T, and ζ. The negativeness of the PDF's in the standard methods lead to small overestimates of the correlation energies. However, other properties which depend directly on the pair correlations would be more reliably estimated using the PDF's generated by the present method. For example, self-interaction corrections as well as nonlocal xc-effects can be treated correctly and self-consistently. Current methods of including nonlocal xc-corrections depend on ''gradient corrections'' using only the value of $g(r=0)$ at ''contact,'' and the large-r behavior from RPA.[47] Another example is the imaginary part of the dielectric function which is directly related to the PDF's via the fluctuation-dissipation theorem, a property exploited in the STLS formulation of the UEG response. Thus Dandrea *et al*. used the Vashista-Singwi form,[18] based on STLS, for constructing a finite-T dielectric function and the corresponding (paramagnetic) $g(r)$.[8] The two parameters A and B contained in the VS $G(q)$ were chosen so that the $q\rightarrow 0$-limit agreed with some estimate of the finite-T compressibility, while the large-q limit, taken to be given by $1-g(r=0)$, was simply set to a fixed value of 0.9. Thus their PDF is evaluated via the following set of equations:

$$G(q)=A(1-e^{Bq^2}), \tag{17}$$

$$\chi(q,\omega)=\chi^0(q,\omega)/[1-V_q(1-G(q))\chi^0(q,\omega)], \tag{18}$$

$$S(q,\omega)=-\mathrm{Im}[\chi(q)]\coth(\beta\omega/2), \tag{19}$$

$$S(k)=\int_{-\infty}^{\infty} S(k,\omega)d\omega/2\pi, \tag{20}$$

$$g(r)=1+(1/n)\mathrm{FT}[S(k)-1]. \tag{21}$$

Here $\chi^0(k,\omega)$ is the noninteracting (Lindhard) response function and the notation ''FT'' indicates a Fourier transformation. The correlation part of the free energy was evaluated from a coupling constant integration over the $g(r)$ obtained from the above procedure. A static $G(q)$ is used in the construction of the dynamic-structure factor $S(q,\omega)$, although a $G(q,\omega)$ is called for. The Dandrea-Ashcroft-Carlsson model is a considerable improvement on the RPA, although some negative-$g(r)$ situations are encountered even for $r_s=2$. A comparison of their results (extracted from their Fig. 14), with the $g(r)$ generated by our method is shown in panel (a) of Fig. 1.

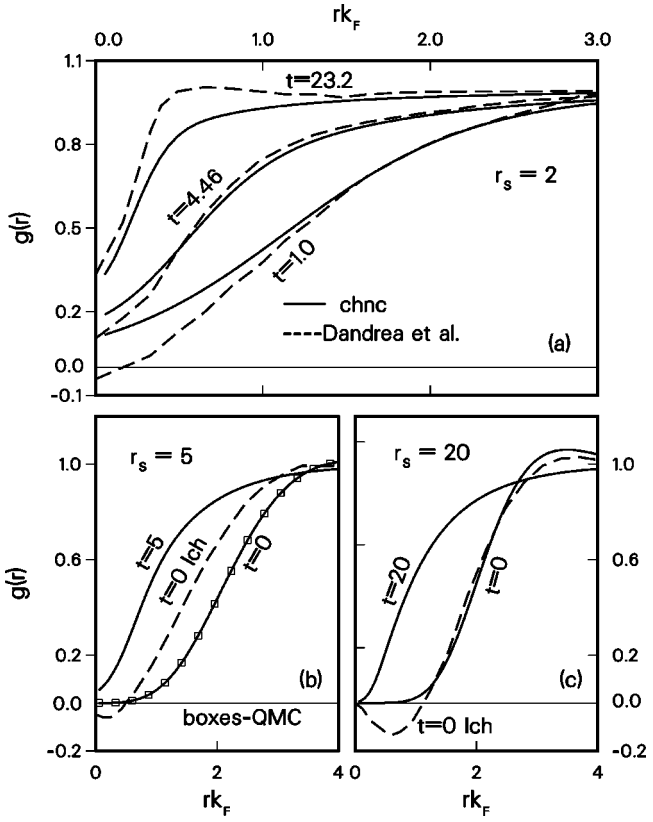

FIG. 1. (a) The $g(r)$ from CHNC (solid lines) are compared with those of Dandrea *et al*., (dashed lines) at $r_s=2$. The temperature $t=T/E_F$. Panel (b) $r_s=5$, CHNC (solid lines) for t=0 and t=5. The $g(r)$ at $t=0$ from Tanaka and Ichimaru (Ref. 22) (dashed line), and from DMC-QMC (Ref. 28), (boxes), are also shown. Panel (c) $r_s=5$, CHNC (solid lines) for $t=0$ snd $t=20$. The $g(r)$ of Tanaka and Ichimaru (Ref. 22), (dashed line) is also shown for $t=0$.

Ichimaru and collaborators have presented several very comprehensive calculational procedures, viz., a method limited to spin-unpolarized systems,[21] based on a direct finite-T version of STLS, and a method based on the modified-convolution approximation (MCA) applicable to spin-polarized systems as well,[22] together with a number of other approximations. Their methods give PDF's which remain positive definite almost up to $r_s\sim 5$. In Fig. 1, panel (b) we show results for other values of r_s and T, as well as a result for $g(r)$ at $r_s=5$ from the MCA results (see their Fig. 4) of Ichimaru *et al*.[22]

The many-electron wave function, suitably integrated over all but a pair of electron coordinates should provide a value of $g(r)$. Given the difficulty of obtaining the full $g(r)$, or the full wave function, many studies have concentrated on the value of $g(r)$ at $r=0$. This has been formulated as a cusp condition on the wave function,[40] a requirement on the large-k limit of the LFC,[41] or in terms of frequency-moment sum rules of the response function.[53] Perdew *et al*.[45] use the value of $g(r=0)$ and the long-range behavior from RPA to construct an interpolation for $g(r)$ for formulating gradient corrections to the local-density approximation (LDA) to DFT. Values of $g(r=0)$ have been calculated using many-body perturbation theory,[42–44] standard double-perturbation theory,[46] and using correlated-determinantal methods. The estimates of $g_{12}(r=0)$ by even two kindered methods like

TABLE I. The value of the electron pair-distribution function at contact, $g_{12}(r=0)$ from various methods. CHNC denotes the classical map-HNC method used in this work.

r_s	1	3	5	10	T/T_F
Yasuhara (Ref. 42)	0.5324	0.1757	0.06656	0.00848	0
vmc (Ref. 28)	0.6740	0.3389	0.1301	0.01116	0
dmc (Ref. 28)	0.5448	0.1843	0.0463	0.00495	0
CHNC	0.4517	0.1038	0.02577	0.00963	0
CHNC	0.4472	0.1068	0.02764	0.00112	1
CHNC	0.5954	0.2252	0.08798	0.00892	5
CHNC	0.6769	0.3192	0.15297	0.02556	10

DMC and VMC tend to be significantly different. In Table I we present the results from the classical-map HNC method, not only for $T=0$, but also for finite T. The value of $g_{12}(r=0)$ increases with temperature, showing that quantum effects become increasingly *important* for the short-ranged behavior as the temperature is increased (see also Fig. 1). That is, classical Debye-Hükel type approximations are not satisfactory for the $g(r)$ at any temperature, for small r.

IV. EXCHANGE-CORRELATION FREE ENERGIES

In this section we present results for the spin-polarized exchange-correlation free energy $f_{xc}(r_s,T,\zeta)$ per electron in Hartree atomic units, at arbitrary temperatures. At $T=0$ the free energy is identical with the internal energy $e_{xc}(r_s,T=0,\zeta)$. At finite temperatures, $e_{xc}=\partial[\beta f_{xc}]/\partial\beta$. Similarly, all the other thermodynamic properties can be calculated from f_{xc} by taking suitable derivatives with respect to density, temperature, and spin polarization. Thus, e.g., denoting the exchange-correlation correction to the chemical potential μ, the pressure P and the compressibility κ by μ_{xc}, P_{xc}, and κ_{xc} respectively, we have

$$\mu_{xc}=\partial[nf_{xc}]/\partial n, \tag{22}$$

$$P_{xc}/n=f_{xc}-\mu_{xc}, \tag{23}$$

$$1/\kappa_{xc}=n^2\partial\mu_{xc}/\partial n. \tag{24}$$

The first of these equations provide μ_{xc} which is identical with the xc-potential of the UEG used in density functional theory. The second equation provides an equation of state for the finite-T electron gas. The temperature $T=1/\beta$, in energy units, refers to the physical temperature and not to the T_{cf} used in the classical-map HNC calculations discussed in the previous sections. The full quantities, e.g., μ, have to be calculated by adding on the noninteracting contributions, e.g., μ_0 to the above xc-contributions. In Ref. 12 we provided parametrizations for the exchange contribution f_x and the ring-sum correlation contribution f_c^{rpa} as separate entities. In the present paper we evaluate and parametrize f_{xc} as a single expression as this ensures that the important cancellations which occur between the two parts are better preserved in the parameter-fitting process. If desired, the correlation contribution f_c at finite T can be obtained from the f_{xc} given here by subtracting f_x, given in Eq. (42) of Ref. 12. The latter is good for $T/T_F\geqslant 0.2$ and does not contain $T^2\log T$-type terms.

TABLE II. A comparison of $-E_c(\zeta=1,T=0)/n$, the negative of the fully spin-polarized correlation energies per electron (a.u.), $\zeta=1$, from the classical map (CHNC) and other methods at $T=0$. The Fermi energy is E_F.

r_s	1	3	5	10
T_q/E_F	0.76805	0.89392	0.99265	1.1980
CHNC	0.03235	0.02157	0.01680	0.011124
CA (Ref. 31)	0.03160	0.02006	0.01551	0.01051
DMC (Ref. 28)	0.02921	0.01869	0.01482	0.01034
VMC (Ref. 28)	0.02634	0.01814	0.01464	0.01020
Lan (Ref. 25)	0.02735	0.01740	0.01355	0.00930
KP (Ref. 26)	−0.03270	0.01840	0.01335	0.00855

A. Results at $T=0$

The *paramagnetic* xc-energy $E_{xc}(r_s,T=0,\zeta=0)$, $r_s\leqslant 10$, is the input to the theory used in determining the temperature T_q. Using the so obtained T_q we can repeat the calculation at any arbitrary spin polarization and obtain the spin-polarized $g_{ij}(r)$ and $E_{xc}(r_s,T=0,\zeta)$. The resulting ζ-dependent energies show a slight overestimate over the QMC results, while other methods on the whole show an underestimate (see Table II). Here it should be noted that the earlier Ceperley-Alder results,[27] VMC, and DMC show a spread of about 5% at $r_s=10$, $\zeta=0$, and 3% at $\zeta=1$. At $r_s=1$ these QMC uncertainties become 11% and 18% at $\zeta=0$ and 1, respectively. If we exclude the older Ceperley-Alder QMC data and compare only the Ortiz-Ballone VMC and DMC data, the spreads become halved.

It is usual to describe the $T=0$ spin-polarized correlation energies in terms of a spin-polarization function $\Gamma(r_s,\zeta)$ given by

$$\varphi(r_s,\zeta)=\frac{E_c(r_s,\zeta)-E_c(r_s,0)}{E_c(r_s,1)-E_c(r_s,0)}. \tag{25}$$

Our results can be accurately fitted to the form:

$$\varphi(r_s,\zeta)=\frac{(1+\zeta)^\alpha+(1-\zeta)^\alpha-2}{2^\alpha-2}, \tag{26}$$

where α is a function of r_s given by

$$\alpha(r_s)=\frac{a+br_s}{1+cr_s} \tag{27}$$

with $a=0.978772$, $b=0.322323$, and $c=0.247303$. The energies are in Hartree atomic units and the fit has an average error of 4.6×10^{-4} a.u., while the maximum error is 8.8×10^{-4} a.u., for the range $1\leqslant r_s\leqslant 10$. The frequently used Hartree-Fock spin-polarization function is independent of r_s, with $\alpha=4/3$. Typical values of α appearing in our fit are found to be 1.042 and 1.213 at $r_s=1$ and 10, respectively.

Our numerical estimate of the $T=0$, $\zeta=0$, $E_c(r_s,0)$ for up to $r_s=10$ is the same as that of Ortiz and Ballone since T_q

TABLE III. Parameters of the functional form of $f_{xc}(r_s,T)$ of Eq. (28), for the unpolarized UEG, obtained from CHNC.

k	$a_{1,k}$	$b_{1,k}$	$c_{1,k}$	$a_{2,k}$	$b_{2,k}$	$c_{2,k}$	ν_k	r_k
1	5.6304	−2.2308	1.7624	2.6083	1.2782	0.16625	1.5	4.4467
2	5.2901	−2.0512	1.6185	−15.076	24.929	2.0261	3.0	4.5581
3	3.6854	−1.5385	1.2629	2.4071	0.78293	0.095869	3.0	4.3909

was evaluated to fit the DMC-QMC data up to $r_s=10$. But CHNC allows us to make predictions for $\zeta\neq 0$ and also for $r_s>10$. Representative values of various quantities obtained from CHNC and other methods are given in Table II.

B. Results at finite temperatures

At finite temperatures, the Helmholz free energy per particle, $f_{xc}(r_s,T,\zeta)$, is obtained from the coupling-constant integration over the distribution functions, while the internal energy per particle, e_{xc}, is obtained at zero temperature. We first consider the paramagnetic case.

1. Paramagnetic UEG at finite T

The finite-T xc-free energy per electron, $f_{xc}(r_s,T)$, is the object of interest. Our results for the unpolarized electron liquid obtained from our calculations can be accurately represented by the form:

$$f_{xc}(r_s,T)=(e_{xc}(r_s,0)-P_1)/P_2, \tag{28}$$

$$P_1=(A_2u_1+A_3u_2)T^2+A_2u_2T^{5/2}, \tag{29}$$

$$P_2=1+A_1T^2+A_3T^{5/2}+A_2T^3, \tag{30}$$

$$u_1=\pi n/2, \tag{31}$$

$$u_2=2\sqrt{(\pi n/3}, \tag{32}$$

$$\ln A_k(r_s)=\frac{y_k(r_s)+\beta_k(r_s)z_k(r_s)}{1+\beta_k(r_s)}, \tag{33}$$

$$y_k(r_s)=\nu_k\ln r_s+\frac{a_{1,k}+b_{1,k}r_s+c_{1,k}r_s^2}{1+0.2r_s^2}, \tag{34}$$

$$z_k(r_s)=r_s\frac{a_{2,k}+b_{2,k}r_s}{1+c_{2,k}r_s^2}, \tag{35}$$

$$\beta_k(r_s)=\exp\left(\frac{r_s-r_k}{0.2}\right). \tag{36}$$

The $e_{xc}(r_s,0)$ appearing in the first of these equations is the usual paramagnetic xc-energy per electron at zero temperature. The values of the fit parameters are given in Table III. The temperature T and f_{xc} are in Hartree atomic units. The density n and r_s are in atomic units. The precision of the fit, measured with respect to the 77 data points of the set $r_s=1,2,3,4,5,8,10$, $T/E_F=0$, 0.25,0.50,1.0,1.5,2,3,4,5, 10, is such that the mean relative error is 0.0035, while the maximum relative error is 0.012. This fit has the following properties:

(1) It gives the QMC xc-energy at $T=0$, where we have used the Ortiz-Ballone E_c fitted to the Perdew-Zunger form, together with the $T=0$ exchange energy.

(2) The second term in the small-T expansion of $f_{xc}(r_s,T)$ goes as T^2. It automatically satisfies the condition of cancellation of the $T^2\ln T$ terms which exist separately in the exchange and correlation parts of $f_{xc}(r_s,T)$.

(3) The high temperature asymptotic expansion has two exact leading terms: the Debye correlation term (proportional to $T^{-1/2}$), and the exchange term (proportional to T^{-1}). These constraints define the density-dependent functions u_1 and u_2.

A comparison of $f_{xc}(r_s,T)$ obtained from the classical-map HNC and some of the other approximations is shown in Fig. 2. Figure 3 shows only the correlation part of the free energy. Comparison between these two figures shows the rather strong cancellation between the exchange and correla-

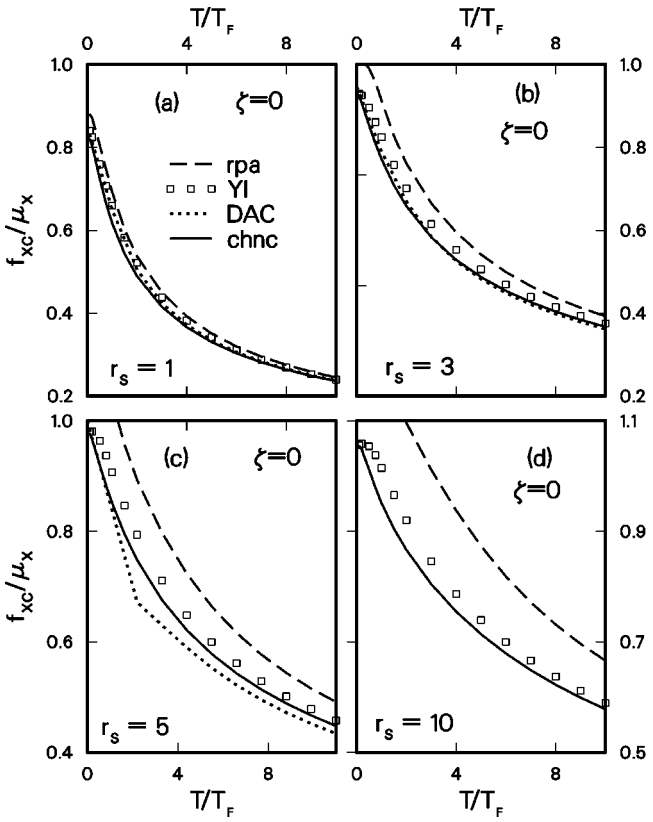

FIG. 2. The xc-free energy per electron, f_{xc}, in units of $\mu_x=-k_F/\pi$, for the unpolarized electron liquid at $r_s=1$, 3, 5, and 10, as a function of the temperature T in units of $T_F=k_F^2/2$. Panels (a) and (b) show results from CHNC (solid lines), RPA (dashed lines), Iyetomi and Ichimaru (Ref. 23) (boxes), and Dandrea *et al.* (Ref. 8) (dotted line). In panels (c) and (d) we display CHNC, Iyetomi and Ichimaru, and the RPA result.

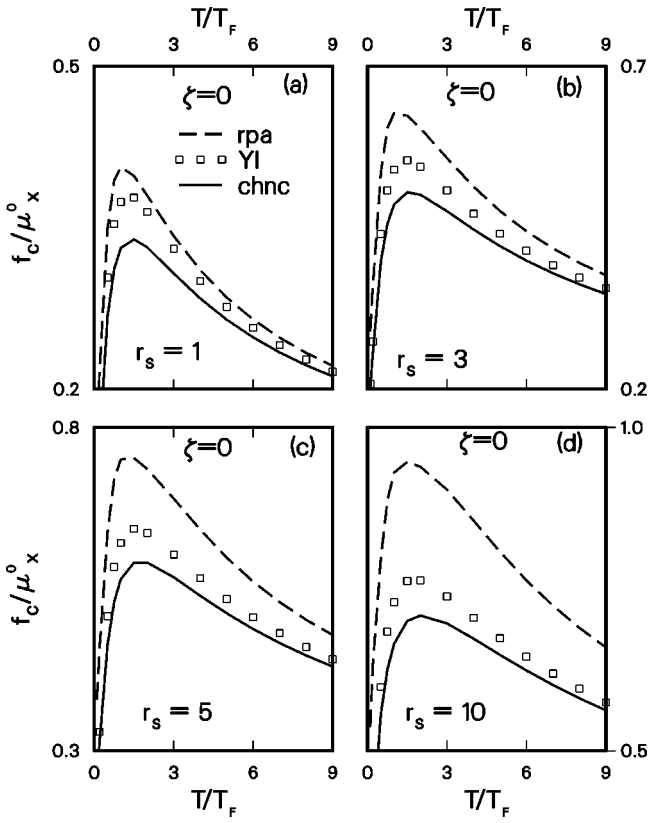

FIG. 3. The correlation contribution to the free energy per electron, f_c, in units of $\mu_x=-k_F/\pi$, for the unpolarized electron liquid at $r_s=1$, 3, 5, and 10, as a function of the temperature T in units of $T_F=k_F^2/2$. Panels show results from CHNC (solid lines), RPA (dashed lines), and Iyetomi and Ichimaru (Ref. 23) (boxes), at $r_s=1$, 3, 5, and 10. Comparison of this with the Fig. 2 shows the strong cancellations between the exchange and correlation parts for $T/T_F<3$.

tion parts, for $T/T_F<3$. The $\zeta=0$ rows in Table IV provides a set of representative values for the unpolarized UEG, useful for direct comparison where necessary.

In Fig. 4 we present results for the xc-bulk modulus (inverse of the xc-compressibility κ_{xc}) as well as the xc-

TABLE IV. Typical values of the negative xc-free energy per particle, $-f_{xc}(r_s,T,\zeta)$, obtained from the classical map (CHNC).

ζ	$T/E_F\rightarrow$	0.4	1.0	4.0	10
	$r_s=1$				
0.0		0.4579	0.3766	0.2234	0.1441
0.6		0.4940	0.4054	0.2363	0.1502
1.0		0.5623	0.4571	0.2593	0.1609
	$r_s=3$				
0.0		0.1773	0.1570	0.1076	0.0747
0.6		0.1861	0.1638	0.1108	0.0763
1.0		0.2025	0.1760	0.1165	0.0793
	$r_s=6$				
0.0		0.0980	0.0896	0.0667	0.0488
0.6		0.1014	0.0921	0.0679	0.0494
1.0		q0.1077	0.0965	0.0700	0.0505

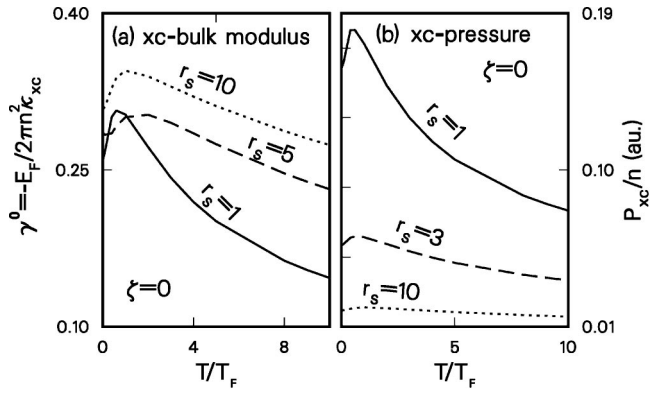

FIG. 4. Panel (a). The xc-bulk modulus, given as $\gamma^0=-E_F/(2\pi n^2\kappa_{xc})$, where κ_{xc} is the xc-compressibility and n is the density, calculated using CHNC is displayed in for $r_s=1$, 5, and 10. Panel (b). The exchange-correlation contribution to the pressure, $p_{xc}/n=f_{xc}-\mu_{xc}$ calculated using CHNC is displayed. Our results of (a) and (b) are in good agreement with those obtained from Iyetomi and Ichmaru (not displayed) (Ref. 23).

pressure P_{xc}. The former is scaled to define a γ^0 which corresponds to the $k=0$ limit of the LFC, but is derived from the xc-free energy differentiated twice with respect to the density [see Eq. (22)]. Both γ^0 and P_{xc} agree very well with the values obtained from the free-energy parametrization given by Iyetomi and Ichimaru (Ref. 23).

2. Results for the finite-T spin-polarized UEG

We consider the finite-T xc-free energy of the polarized UEG, with n_1 the majority-spin density, while $n=n_1+n_2$, and $\zeta=(n_1-n_2)/(n_1+n_2)$. As already remarked, we work with f_{xc} rather than with f_x and f_c. The polarization function is defined as

$$\varphi(r_s,T,\zeta)=\frac{f_{xc}(r_s,T,\zeta)-f_{xc}(r_s,T,0)}{f_{xc}(r_s,T,1)-f_{xc}(r_s,T,0)}. \tag{37}$$

In the zero-T case one has

$$e_x(r_s,\zeta=1)=2^{1/3}e_x(r_s,\zeta=0), \tag{38}$$

where $e_x(r_s,\zeta=1)$ is the exchange energy per electron. Hence, by analogy we write

$$f_{xc}(r_s,T,\zeta=1)=2^B f_{xc}(r_s,T,\zeta=0), \tag{39}$$

where B is a function $B(r_s,T)$ to be determined. In analogy with the $T=0$ case, we assume that $\varphi(r_s,T,\zeta)$ has the same functional form as Eq. (26), but the exponent α is now a function of r_s and T. This leads to the following form for the spin-dependent xc-free energy where we have used $t=T/E_F$:

$$f_{xc}(r_s,T,\zeta)=f_{xc}(r_s,T,0)[1+(2^B-1)\varphi(r_s,T,\zeta)], \tag{40}$$

$$\varphi(r_s,T,\zeta)=\frac{(1+\zeta)^\alpha+(1-\zeta)^\alpha-2}{2^\alpha-2}, \tag{41}$$

$$\alpha(r_s,T)=2-g(r_s)e^{-t\lambda(r_s,t)}, \tag{42}$$

TABLE V. Values of the parameters used in the functional form of $f_{xc}(r_s,T,\zeta)$ of Eq. (40), for the spin-polarized UEG, obtained from CHNC.

k	p_k	q_1	s_k	u_k	σ_k
1	0.653676	0.166896	−0.373864	0.472245	1.000000
2	−0.157510	−0.308756	−0.144853	2.495400	2.236068
3	0.190535	0.691258	−0.890943	5.656750	3.162278

$$g(r_s)=(g_1+g_2r_s)/(1+g_3r_s), \tag{43}$$

$$\lambda(r_s,t)=1.089+0.70t\sqrt{r_s}, \tag{44}$$

$$\frac{1}{B(r_s,T)}=\sum_{i\neq j\neq k}^{1\leqslant i,j,k\leqslant 3}\frac{(\sqrt{(r_s)}-\sigma_i)(\sqrt{(r_s)}-\sigma_j)}{D_k}, \tag{45}$$

$$D_k=\frac{p_k+q_kt^{1/3}}{1+s_kt^{1/3}+u_kt^{2/3}}. \tag{46}$$

The values of the three coefficients in $g(r_s)$ are $g_1=0.644\,291$, $g_2=0.063\,944\,3$, and $g_3=0.249\,611$. The coefficients σ_k,p_k,q_k,s_k, and u_k, $k=1,2,3$ appearing in the above equations are given in Table V.

The parametrized form of the free energy may be used to obtaining other thermodynamic quantities as well as the spin-dependent xc-potentials of DFT by suitable manipulations. The spin-polarized RPA xc-free energy, viz., f_{xc}^{rpa}, can be evaluated from the RPA-grand potential $\Omega(r_s,T,\zeta)$ reported by Kanhere *et al.*[13] In the work of Tanaka and Ichimaru,[22] the spin-polarization effects have been treated using the Hartree-Fock form of φ. The results of Dandrea *et al.* (Ref. 8) are limited to the paramagnetic case. Representative values of $f_{xc}(r_s,T,\zeta)$ are given in Table IV.

C. Exchange-correlation potentials

An important derived property of $f_{xc}(r_s,T,\zeta)$ is the xc-potential which enters in the Kohn-Sham equations. In the unpolarized case, the xc-potential $V_{xc}(n)$ is the density derivative $d[nf_{xc}(n)]/dn$. Thus it is identical with the xc-chemical potential μ_{xc}. When we have a spin-polarized system, the densities n_σ, $\sigma=1,2$ for the up-spin and down-spin species, are treated as independent variables, with the total density $n=n_1+n_2$. The two-component system has four PDFs, viz., $g_{ij}(r)$, and hence one should formally define a *matrix* of xc-potentials based on the derivatives of the energy contributions of the four pair-distribution functions. However, it is customary in spin-density functional theory (SDFT) to just define two spin xc-potentials by

$$V_{xc\sigma}=\partial[nf_{xc}(n_1,n_2)]/\partial n_\sigma. \tag{47}$$

Here the derivative with respect to the density of one of the spin species (e.g., n_1) is taken while the density of the other component (e.g., n_2) is held fixed. This approach assumes a constant direction of spin polarization and is not immediately applicable to the spin-density-functional calculations of inhomogeneous systems where the direction of spin polarization varies as a function of position. In such situations it is best to use the full matrix of distributions functions $g_{ij}(r)$ to construct a matrix of xc-potentials. An alternative method, frequently used within the local-spin-density approximation (LSDA) is the approach introduced by Kübler *et al.*,[48] where the spin-quantization axis is rotated to locally diagonalize the spin-density matrix. In this study we will present some results for $V_{xc\sigma}$ in the form used in LSDA. In Table VI a representative set of values of $V_{xc\sigma}$ is given. In Fig. 5 we compare our strong-coupling estimate with the RPA estimate of $V_{xc\sigma}$ given by the Baton-Rouge group.[49] It is clear that the RPA overestimates the correlations, as expected. Thus, for $r_s\sim 5$, the overestimate is about 10–20%. Also, the polarization dependence of the strong-coupling result changes character around $T/T_F\sim 2$. It is seen, especially in panel (b), that the polarization dependence is quite weak for $\zeta>0.4$, while the highest sensitivity is near $\zeta\sim 0$.

TABLE VI. Typical values of the negative of the spin-polarized xc-potential (Hartree a.u.) for majority-spin electrons. $-V_{xc\sigma}(r_s,T,\zeta)$, obtained from the classical map (CHNC).

ζ	$T/E_F\rightarrow$	0.4	1.0	4.0	10
	$r_s=1$				
0.0		0.6383	0.5492	0.3398	0.2208
0.4		0.7108	0.6090	0.3679	0.2341
0.8		0.7722	0.6613	0.3948	0.2472
	$r_s=5$				
0.0		0.1517	0.1429	0.1098	0.08091
0.4		0.1607	0.1499	0.1132	0.08272
0.8		0.1686	0.1562	0.1166	0.08451

V. LOCAL-FIELD CORRECTIONS

The response function of the electron gas is intimately connected with the PDF's, as already discussed within the context of Eq. (17). The usual approach is to find an LFC from perturbation theory or from equations of motion etc., and then use the fluctuation dissipation theorem to get at the PDF's self-consistently, if possible. As we know, such methods are extremely difficult to carry out successfully to obtain a positive definite $g(r)$. In contrast, in our approach we al-

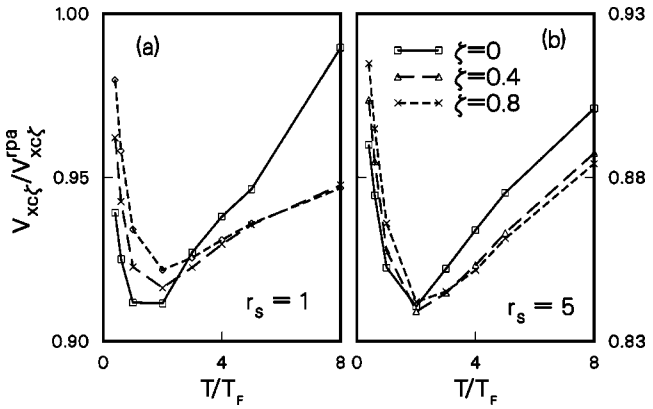

FIG. 5. The spin-polarized xc-potential $V_{xc\sigma}(r_s,t,\zeta)$ in units of the corresponding RPA value is shown for the majority-spin component, $\sigma=1$. Here $t=T/T_F$, $\zeta=(n_1-n_2)/(n_1+n_2)$. The spin-polarized RPA potentials are from Kanhere *et al.* (Refs. 13 and 49).

ready have the $g(r)$ and so proceed to evaluate the LFC and the interacting response function from the $g(r)$.

The response $\chi(k,\omega)$ of the interacting UEG is usually written in terms of a reference $\chi^0(k,\omega)$ and an LFC denoted by $G(k,\omega)$. Such a form ensures that the *f*-sum rule is automatically satisfied for any physically sensible $G(k,\omega)$, including the static form. The simplest static form, $G(k)$, is identical with $G(k,0)$ at $k=0$, and begins to differ from $G(k,\omega)$ as k increases. In general, the $G(k,\omega)$ for ω smaller than the plasma frequency ω_p behaves like a static quantity. Hence the use of a static form $G(k)$ is often adequate. The main thrust of STLS,[18] GT,[15] UI,[50] FHER,[51] and others has been to provide the $G(k)$ as a function of r_s at $T=0$. Even though UI begins as a basic theory, it actually relies on fit parameters constraining the $G(k)$ to fits to Monte Carlo E_{xc} and derivatives, and to Yasuhara's $g(0)$,[42] i.e., it invokes quantities outside UI theory. FHER take the parametric form of the UI's LFC and successfully fit it to available theoretical results (at $T=0$) for the UEG, using an ample array of parameters to handle the known sum rules and other physical requirements. However, there is no clear way of ensuring that the LFC of FHER corresponds to the physical $g(r)$. Relating the LFC to the $g(r)$ in the quantum case proceeds via an integration over ω, as in Eq. (20). This requires a knowledge of $G(k,\omega)$ and not just $G(k)$. By contrast, in the classical case no integration over ω is required.

The only ''fit'' parameter of the present model is T_q. Further, since the PDF's have been evaluated for a classical fluid, we can use the properties of classical distribution functions to evaluate the LFC which is expressible in terms of the direct correlation functions or structure factors of the interacting and zeroth-order systems. Thus consider the simplest LFC, viz., $G(k)$, for a one-component fluid:

$$V_{cou}(k)G(k)=V_{cou}(k)+1/\chi(k)-1/\chi^0(k). \tag{48}$$

For a classical fluid, $\chi(k)$ is directly related to the structure factor:

$$S_{ij}(k)=-(1/\beta_{cf})\chi_{ij}(k)/(n_i n_j)^{1/2}. \tag{49}$$

Hence, for the paramagnetic case:

$$V_{cou}(k)G(k)=V_{cou}(k)-\frac{T_{cf}}{n}\left[\frac{1}{S(k)}-\frac{1}{S^0(k)}\right]. \tag{50}$$

Note that here we have used the temperature of the interacting system, viz., T_{cf} with $S^0(k)$ itself. We believe that this is equivalent to using an interacting $\chi^0(k)$ as the reference response function.[52,53] In these expressions the $\chi^0(k)$ and $S^0(k)$ are based on a Slater determinant, while the Lindhard function is applicable to the noninteracting case without antisymmetrization of the wave function. We display in Fig. 6 the LFC for $r_s=5$, for several values of the temperature $t=T/T_F$.

As already mentioned in the context of the work of Dandrea *et al.*, the two-parameter Vashista-Singwi LFC, given by

$$G(q)=A(1-e^{-Bq^2}),\quad q=k/k_F, \tag{51}$$

has sometimes been used as a model for the LFC, even at finite temperatures, since A and B can be determined by the compressibility sum rule which defines the limit of $G(q)/q^2$ for $q\to 0$, and the $q\to\infty$ limit of $G(q)$. Thus

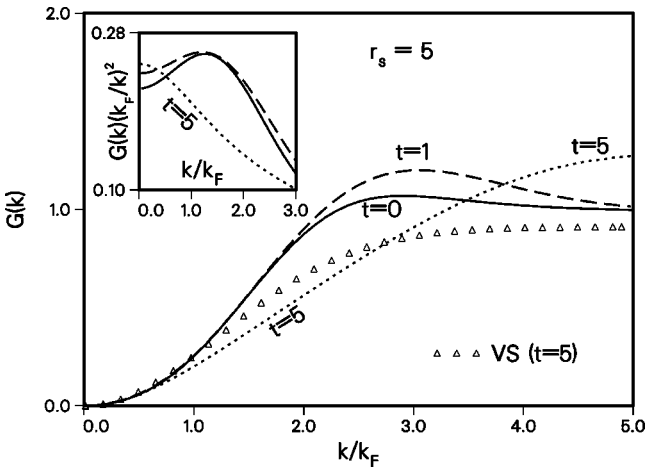

FIG. 6. The static local field correction (LFC), $G(q)$ calculated from CHNC at $r_s=5$ and $T/T_F=t=0$, 1, and 5 are displayed. The data points (triangles) are for a finite-T LFC based on the Vashista-Singwi two-parameter form where the $q\to 0$ and $q\to\infty$ are fitted to the CHNC γ^0, (see Table VII), and $1-g(0)$ (see Table I). The inset shows the small-q behavior of $G(q)/q^2$, showing that the hump in the LFC for $q\sim 1.5-2$ has disappeared for the high temperature case. Comparisons of the LFC from CHNC at $t=0$ with other models was given in our Ref. 35.

$$AB=\gamma^0, \tag{52}$$

$$\gamma^0=G(q)/q^2|_{q=0} \tag{53}$$

$$=-\frac{E_F}{2\pi n}\frac{1}{\kappa_{xc}}, \tag{54}$$

$$A=G(q\to\infty)=1-g(0). \tag{55}$$

The xc-compressibility κ_{xc} at any temperature is known from our parametrized form of the free energy $f_xc(r_s,T,\zeta)$ (see Fig. 4). In Table VII we give a set of values of γ^0 for convenience. Similarly, $g(0)$, the value of the PDF, at contact is also known from the CHNC procedure (see Table I). Hence we can construct finite-temperature two-parameter ζ-dependent VS-LFC's. A result is shown for the paramagnetic case, in Fig. 6 by triangles, together with CHNC-LFC (dotted line) for $T=5E_F$ and $r_s=5$. The VS form provides a poor representation of the intermediate-k region. This was

TABLE VII. Typical values of γ^0, the $q=0$ limit of the $G(q)/q^2$ function where $G(q)$ is the local-field correction to the response function [see Eq. (52), and Fig. 4(a)]. The γ^0 values are derived from the CHNC xc-free energy, $f_{xc}(r_s,T,\zeta=0)$.

$T/E_F\to$ $r_s\downarrow$	0.4	1.0	4.0	10
1	0.3008	0.3031	0.2194	0.1468
3	0.2908	0.3034	0.2639	0.2008
5	0.2851	0.3005	0.2851	0.2316
8	0.3160	0.3254	0.3044	0.2574
10	0.3285	0.3451	0.3203	0.2739

already noted many years ago by Sham.[54] He pointed out that the VS and related methods do not capture the exchange effects which determine the LFC near $2k_F$, for $T=0$. The model LFC can be easily improved by introducing an extra level of parametrization such that $G(q)\sim 1$ for some intermediate wave vector $2k_{Ft}$. The latter should be such that it becomes $2k_F$ at $t=0$ and increase with temperature. However, we shall not examine such an approach any further, as it does not guarantee a positive definite $g(r)$. It may however prove to be useful when the full CHNC procedure is not needed.

It should be remarked that the LFC's based on a χ_I^0 calculated with the interacting-density distribution tend to a constant for large k, viz., $G(k,0)\to 2(1-g(0))/3$, while $G(k)\to 1-g(0)$. If we look at some of the $T=0$ theories, the theory of UI is based on a χ_I^0, but in practice the Lindhard χ^0 is used. The fitted $G(k,0)$ of FHER is built to behave like k^2 at large k, being an LFC based on the Lindhard form.[53] The large-k limit of the LFC obtained from the CHNC can be investigated as follows. The large-k limit of $S(k)$, at density n and fractional composition $x=1/2$ for the paramagnetic case is given by

$$S(k)=1-\frac{4\pi}{k^4}nx\left[2\frac{d}{dr}h_{12}(r)\right]_{r=0}, \tag{56}$$

$$\frac{dg_{12}(r)}{dr}=-\frac{d}{dr}e^{-\beta_{cf}V_{cou}(r)}, \tag{57}$$

$$g(0)=g_{12}(0)/2. \tag{58}$$

Now, using the above limiting forms and the diffraction form of $V_{cou}(k)$ in Eq. (50) it is found that

$$G(k)|_{k\to\infty}=1-g(0). \tag{59}$$

It should be noted that the diffraction potential used here does not lead to the Kimball relation $dg(r)/dr|_{r=0}=g(0)$ but to the form $dg(r)/dr|_{r=0}=g(0)(\beta_{cf}/2\lambda^2)$ if the contributions from the nodal term at $r=0$ are ignored. In the usual derivations of the Kimball relation it is often assumed that the strongly repulsive Coulomb potential at $r=0$ implies that *only* the interacting pair of electrons is present, and that the effect of the other electrons could be neglected. However, the diffraction form of the potential is weak at $r=0$ and *does not* exclude the presence of other electrons. Hence the usual form of the Kimball relation is not relevant to us. Also, it is not clear if the very large-k limit is meaningful for $k>1/\lambda_{th}$. In practice, the behavior of the LFC for large-k is not important since the response function $\chi(k,\omega)$ as well as $\chi^0(k,\omega)$ decay rapidly for large k.

VI. APPLICATION OF THE XC-POTENTIALS TO A FINITE-T KOHN-SHAM CALCULATION

One of the most important applications of the xc-free energies and potentials is to finite-T Kohn-Sham calculations. We consider a typical system, namely, an Al^{13+} nucleus immersed in an electron gas of half the normal density of solid aluminum, and at a temperature of 15 eV. In such calculations the neutralizing background of the electron gas is modified to have a cavity whose radius is equal to the Wigner-Seitz radius of the Al ion, and the nucleus is placed at the center of the Wigner-Seitz sphere.[5,55] Since the system has spherical symmetry, the Kohn-Sham equations reduces to a radial equation which has to be solved iteratively, since the Hartree potential and also the xc-potential depend implicitly on the electron-density distribution. Our aim is to assess the difference between the CHNC xc-potential and, for instance, the Iyetomi-Ichimaru (YI) xc-potential. For this purpose we limit ourself here to a spin-unpolarized DFT calculation in the local-density approximation. We examine the electronic structure of the ''average atom'' where the electron occupations are assumed to be given by the Fermi distribution at the given temperature.[55,56]

The K-S bound states obtained by the two methods, CHNC and YI, respectively, are at energies (in Rydbergs) of -115.044 and -110.199 for the $1s$ level, -7.86214 and -7.53968 for the $2s$ level. The outermost level, the $2p$-state, has an energy (Ry) of -5.05646 and -4.81116 from CHNC and YI, respectively. Similar proportionate changes are seen in the phase shifts of the continuum states. Thus it is clear that the xc-potentials should have a significant impact, especially in determining the regimes of plasma phase transitions, finite-T magnetic transitions,[6] as well as in the accurate determination of ionization balance and transport properties. A more complete study of these phenomena using fully nonlocal, self-interaction-corrected, spin-dependent methods is now emerging since the $g_{ij}(r)$ may be easily evaluated and directly used in the Kohn-Sham calculations, using the CHNC methods presented in this study.

VII. CONCLUDING DISCUSSION

We have presented the application of the classical mapping of the Coulomb interactions using the HNC procedure to the finite-T uniform electron gas. It was shown in a previous publication that the method accurately reproduces the pair distributions and xc-energies of the $T=0$ quantum-electron fluid. Here we examined our results by comparison with other published approaches. The methods proposed by Ichimaru and collaborators, and also by Dandrea *et al.*, lead to $g(r)$ which are in reasonable agreement with the CHNC results whenever their $g(r)$ remain positive definite. In other cases, when their $g(r)$ contain negative regions, the positive, large-r part of their PDF's seem to fall into agreement with our results. The exchange-correlation free energies f_{xc} calculated by the CHNC show that the forms proposed by Ichimaru *et al.* provide good estimates of the free energies and derived properties, even though there is some overestimate in the correlation effects, especially in the regimes where the traditional methods give negative PDF's. Currently there are no quantum Monte Carlo results for the finite-T uniform electron gas that we can use for comparison. We have presented an easy to use parametrization of $f_{xc}(r_s,T,\zeta)$ fitted to a large data base with r_s and T/T_F up to 10, and ensuring the correct asymptotic behaviors. The parametrization is believed to be sufficiently accurate for obtaining derived properties like the pressure, compressibility and the spin-dependent xc-potentials of density functional theory at finite T. The computer programs for generating the PDF's, the $f_{xc}(r_s,T,\zeta)$ and related properties are available online to

other workers via web access.[57]

The present approach, based on the CHNC scheme, provides a unified formulation of the thermodynamics and dielectric response of the uniform interacting-electron fluid (or other Coulombic-Fermion fluids) at finite temperatures and for general values of spin polarization and coupling strength, with a minimum of assumptions.

APPENDIX: PHYSICAL MEANING OF THE "CLASSICAL-FLUID TEMPERATURE"

The temperature of the classical fluid, T_{cf}, which is used to calculate the distribution functions and excess free energies of the electron fluid at the physical temperature T was modeled using the quadratic interpolation:

$$T_{cf}^2 = T_q^2 + T^2. \tag{A1}$$

In density functional theory, the kinetic energy is described by noninteracting electrons at the interacting density. Let us assume that the meanvalue E_{kin} of the kinetic energy operator can be described by some classical temperature T_{clas}. Restoring the k_B factors for the sake of clarity, we then have,

$$E_{kin} = \frac{3}{2} k_B T_{clas} = \frac{\sqrt{2}\pi^{-2}(k_B T)^{5/2} I_{3/2}(\beta\mu)}{\sqrt{2}\pi^{-2}(k_B T)^{3/2} I_{1/2}(\beta\mu)}. \tag{A2}$$

Here $I_{1/2}(x)$, $I_{3/2}(x)$ are the usual Fermi integrals. The numerator is the kinetic-energy density and the denominator is the electron density. The denominator can be expressed in terms of the Fermi temperature since

$$(k_B T)^{3/2} I_{1/2}(\beta\mu) = 2/3 (k_B T_F)^{3/2}. \tag{A3}$$

Hence we have

$$T_{clas}/T_F = (T/T_F)^{5/2} I_{3/2}(\beta\mu). \tag{A4}$$

Let us define $X(T) = T_{clas}/T_F$. The quadratic interpolation that we have used is of the form:

$$Y(T) = T_{cf}/T_F = \sqrt{A^2 + (T/T_F)^2}. \tag{A5}$$

The constant $A = X(T)|_{T\to 0}$ is 2/5, and is independent of r_s. It is easily shown numerically that the ratio $Y(T)/X(T)$ is always very close to unity, with a maximum error of -6% around $T/T_F = 0.5$. This shows that the chosen functional form (surd of a sum of quadratics) describes the quantum-kinetic energy (which involves a ratio of Fermi integrals) very well. In our quadratic interpolation we do not use a constant A, but an r_s-dependent quantity T_q/T_F, obtained by fitting to the UEG at $T=0$.

*Electronic mail address: chandre@cm1.phy.nrc.ca

[1] H. M. Van Horn, Science **252**, 384 (1991).

[2] G. D. Mahan, *Many-Particle Physics* (Plenum, New York, 1981).

[3] D. H. E. Dubin, Phys. Rev. A **42**, 4972 (1990); W. L. Slattery, G. D. Doolen, and H. E. DeWitt, Phys. Rev. A **26**, 2255 (1982); J-P. Hansen, Phys. Rev. A **8**, 3096 (1973); S. G. Brush, H. L. Sahlin, and E. Teller, J. Chem. Phys. **45**, 2102 (1966).

[4] W. Kohn and L. J. Sham, Phys. Rev. **140**, A1133 (1965).

[5] M. W. C. Dharma-wardana and F. Perrot, in *Density Functional Theory*, edited by E. K. U. Gross and R. M. Dreizler (Plenum, New York, 1995), p. 635.

[6] S. Ichimaru, Phys. Rev. Lett. **84**, 1843 (1999); D. P. Young, D. Hall, M. E. Torelli, Z. Fisk, J. L. Sarro, J. D. Thompson, H.-R. Ott, S. B. Oeroff, R. G. Goodrich, and R. Zysler, Nature (London) **397**, 412 (1999).

[7] R. J. Hemley, Nature (London) **404**, 240 (2000), and references therein.

[8] R. B. Dandrea, N. W. Ashcroft, and A. E. Carlsson, Phys. Rev. B **34**, 2097 (1986). Our implementation of Eq. (A5) for the parametrized form of f_{xc} of this publication does not lead to reasonable results for $r_s > 3$; we conjecture a possible typographical error in their Table I. We thank Professors Carlsson and Ashcroft for private communications.

[9] S. Hong and G. D. Mahan, Phys. Rev. B **53**, 1215 (1996).

[10] U. Gupta and A. K. Rajagopal, Phys. Rev. A **22**, 2792 (1980).

[11] M. W. C. Dharma-wardana and R. Taylor, J. Phys. C **14**, 629 (1981).

[12] F. Perrot and M. W. C. Dharma-wardana, Phys. Rev. A **30**, 2619 (1984).

[13] D. G. Kanhere, P. V. Panat, A. K. Rajagopal, and J. Callaway, Phys. Rev. A **33**, 490 (1986).

[14] J. Hubbard, Proc. R. Soc. London **243**, 336 (1957).

[15] D. J. W. Geldart and R. Taylor, Can. J. Phys. **48**, 155 (1970).

[16] M. W. C. Dharma-wardana and R. Taylor, J. Phys. F **10**, 2217 (1980).

[17] F. Green, D. Neilson, and J. Szymański, Phys. Rev. B **31**, 2796 (1985); Tanaka and Ichimaru, Phys. Rev. B **39**, 1036 (1989); Richardson and Ashcroft, Phys. Rev. B **50**, 8170 (1994).

[18] K. S. Singwi, M. P. Tosi, R. H. Lund, and A. Sjölander, Phys. Rev. **176**, 589 (1968).

[19] P. Vashista and K. S. Singwi, Phys. Rev. B **175**, 589 (1972).

[20] M. W. C. Dharma-wardana, J. Phys. C **9**, 1919 (1976).

[21] S. Ichimaru and S. Tanaka, Phys. Rev. A **32**, 1790 (1985).

[22] S. Tanaka and S. Ichimaru, Phys. Rev. B **39**, 1036 (1989).

[23] H. Iyetomi and S. Ichimaru, Phys. Rev. A **34**, 433 (1986).

[24] E. Feenberg, *Theory of Quantum Fluids* (Academic, New York, 1969); C. E. Campbell and J. G. Zabolitzky, Phys. Rev. B **27**, 7772 (1983); T. Chakraborty, Phys. Rev. B **29**, 3975 (1984).

[25] L. J. Lantto, Phys. Rev. B **22**, 1380 (1980).

[26] A. Kallio and J. Piilo, Phys. Rev. Lett. **77**, 4237 (1996).

[27] D. M. Ceperley, *Recent Progress in Many-body Theories*, edited by J. G. Zabolitzky (Springer, Berlin, 1981), p. 262.

[28] G. Ortiz and P. Ballone, Phys. Rev. B **50**, 1391 (1994).

[29] G. Ortiz, M. Harris, and P. Ballone, Phys. Rev. Lett. **82**, 5317 (1999).

[30] S. Moroni, D. Ceperley, and G. Senatore, Phys. Rev. Lett. **75**, 689 (1995).

[31] D. M. Ceperley and B. J. Alder, Phys. Rev. Lett. **45**, 566 (1980).

[32] S. H. Vosko, L. Wilk, and M. Nusair, Can. J. Phys. **25**, 283 (1989).

[33] J. P. Perdew and A. Zunger, Phys. Rev. B **23**, 5048 (1981).

[34] B. Militzer and E. L. Pollock, Phys. Rev. E **61**, 3470 (2000); D. M. Ceperley, Rev. Mod. Phys. **67**, 279 (1995).

[35] M. W. C. Dharma-wardana and F. Perrot, Phys. Rev. Lett. **84**, 959 (2000).

[36] J. M. J. van Leeuwen, J. Gröneveld, and J. de Boer, Physica (Amsterdam) **25**, 792 (1959).

[37] F. Lado, J. Chem. Phys. **47**, 5369 (1967).
[38] F. Lado, S. M. Foiles, and N. W. Ashcroft, Phys. Rev. A **28**, 2374 (1983); Y. Rosenfeld, Phys. Rev. A **35**, 938 (1987).
[39] H. Minoo, M. Gombert, and C. Deutsch, Phys. Rev. A **23**, 924 (1981).
[40] T. Kato, Commun. Pure Appl. Math. **10**, 151 (1957).
[41] J. C. Kimball, Phys. Rev. A **7**, 1648 (1973).
[42] H. Yasuhara, Solid State Commun. **11**, 1481 (1972).
[43] D. J. W. Geldart, Can. J. Phys. **45**, 3191 (1967).
[44] L. Calmels and A. Gold, Phys. Rev. B **57**, 1436 (1998).
[45] K. Burke, J. P. Perdew, and M. Ernzerhof, J. Chem. Phys. **109**, 3760 (1998).
[46] V. A. Rassolov, J. A. Pople, and M. A. Ratner, Phys. Rev. B **59**, 15 625 (1999).
[47] J. P. Perdew and Y. Wang, Phys. Rev. B **45**, 13 244 (1992).
[48] J. Kübler, K.-H. Hóck, J. Sticht, and A. R. Williams, J. Phys. F **18**, 469 (1988); see also L. M. Sandratskii, Adv. Phys. **47**, 91 (1998).
[49] See Ref. 13. As recommended by the authors, rather than using the fit formula given in the appendix of Kanhere *et al*., we have used a tabulation of $V_{xc\sigma}(r_s,T)$ provided to us by Professor Callaway at the time of the publication of Ref. 13.
[50] K. Utsumi and S. Ichimaru, Phys. Rev. B **24**, 3220 (1981).
[51] B. Farid, V. Heine, G. Engel, and L. J. Robertson, Phys. Rev. B **48**, 11 602 (1993).
[52] G. Nicklasson, Phys. Rev. B **10**, 3052 (1974).
[53] A. Holas, in *Strongly Coupled Plasma Physics*, edited by F. J. Rogers and H. E. DeWitt (Plenum, New York, 1987), p. 463.
[54] L. J. Sham, Phys. Rev. B **7**, 4357 (1973).
[55] L. Dagens, J. Phys. F: Met. Phys. **71**, 1167 (1977); F. Perrot, Phys. Rev. E **47**, 570 (1993).
[56] F. Perrot and M. W. C. Dharma-wardana, Phys. Rev. E **52**, 5352 (1995).
[57] Readers who wish to use our results may access some of our codes via web input by following the instructions given in http://www.nrc.ca/ims/qp/chandre/